Vacuum ultraviolet reflectivities of LiF, NaF, and KF†

K. Kameswara Rao, T. J. Moravec, J. C. Rife, and R. N. Dexter
Physics Department, University of Wisconsin, Madison, Wisconsin 53706
(Received 23 June 1975)

High-resolution normal-incidence (9°) reflectivities of lithium-fluoride, sodium-fluoride, and potassium-fluoride single crystals were investigated between 6 and 35 eV at room temperature, 100 and 30 K using a minicomputer-controlled vacuum ultraviolet reflectometer at the Winconsin Synchrotron Radiation Facility. Data were taken on surfaces cleaved and maintained in high vacuum. Reflectivity data were Kramers-Kronig analyzed to yield the dielectric functions of the materials and various energy and temperature derivatives were calculated as an aid to interpretation. In all materials, considerable new structure is reported with broad, general agreement with earlier work on LiF and KF. We report the first reflectivity data between 12 and 35 eV for NaF. Computed values of $-\mathrm{Im}(1/\epsilon)$ were in good agreement with electron-energy-loss experiments of Creuzburg. It is only possible to provide detailed interpretation of optical features in special cases, but a general discussion is provided in the conventional framework.

I. INTRODUCTION

There have been many studies of the optical properties of the alkali halides in the vacuum ultraviolet.[1-7] In particular, the reflectivities of LiF and KF have been studied in their fundamental spectral region at room temperature using conventional light sources.[5,8] The sharp peaks observed in the optical spectra of alkali halides near the fundamental absorption edge are customarily described as due to excitons. In general, it is impossible to resolve within the same energy region the full multiplicity of structure arising from exciton formation in different regions of the Brillouin zone, from the spin-orbit splitting, and from the higher principal quantum numbers of exciton excitations. The problem is particularly obscure in LiF and NaF, where a single rather-broad peak is found at the onset of absorption. Although the optical spectrum of the lightest alkali halide LiF is very simple, its theoretical interpretation is not fully satisfactory. The situation is worse in NaF, for which published broad-range optical constants are not available, and for KF, for which there is an overabundance of spectral features. Our results are not in good accord with unpublished results[9] on NaF which have been quoted elsewhere.

The most comprehensive room-temperature investigation of the reflectivity of LiF is by Roessler and Walker[5] (RW), with which this study is in substantial accord. Although we add a number of features to the list of high-energy optical characteristics, the ϵ_2 spectrum is found at all temperatures studied to be dominated by a strong peak at about 12.6 eV and lesser and broad bands at 14.3, 17.4, and 21.7 eV in ϵ_2. The 12.6-eV peak was identified[5] as a Γ exciton by analogy with other alkali halides, despite its pronounced asymmetry, and the shape of the remaining spectrum led to the conclusion that the band gap at Γ is 13.6 eV. We will present no evidence in conflict with that conclusion.

RW further calculated the energy-loss function and identified peaks at 13.5, 15.6, and 18 eV as due to single-particle excitations and the very strong peak at 24.9 eV as a plasma resonance of valence electrons. Lacking good theoretical band structures they did not attempt to identify optical features with specific locations in the zone but others have since made such identifications.[10,11] In the case of the calculated energy-loss function, the general shape and relative scale were in good agreement with experiment, although the magnitude of the energy loss was not.

Results on the LiF reflectivity by Stephan[12] have been discussed,[11] and these results are very similar to those of RW except for a doublet at 17.4 eV in Stephan's data. We did not confirm the existence of the doublet but were stimulated in these studies by the hope of resolving this or other hidden features of the LiF optical constants by the use of the continuum synchrotron radiation source.

After the initial band-structure calculations of Ewing and Seitz,[13] many band calculations have been performed[10,11,14-24] for LiF placing the similar band features in rather different energy regions. In many cases the band gap is clamped at the assumed value of 13.6 eV, and in other cases the gap is calculated using an assumed potential. A large variation in the results of recent work is indicated in Table I. Energies of primary optical features in ϵ_2 are also listed to illustrate the experimental energy scales. The interband identification is further obscured by the probability of

many-body excitations within the same optical range. Specifically, referring to the calculated band gaps, for those papers[15,16,19,23] which do not assume the gap of 13.6 eV it will be seen that a much smaller gap is calculated in several cases, between 10.6 and 12 eV. We doubt that a band gap of less than 12 eV is compatible with the high transparency of LiF to such energies, but we carefully searched for optical features below the primary reflectivity peak.

In the work of Menzel *et al.*[19] the main peak in ϵ_2 was interpreted as a band-to-band transition near the L point, in contrast to the excitonic interpretation of other investigators. The primary conclusion of their work, namely, that an unusually large matrix element exists for transitions near the L point, may help in the identification of the higher-energy optical features, even if their interpretation is not completely upheld. Furthermore, the 23-eV peak is interpreted as due to the electronic polaron by Devreese *et al.*,[25] to a double exciton or plasmon by Miyakawa,[26] and to a plasmon absorption by RW. We hoped to clarify these problems in LiF by performing lower-temperature and perhaps higher-resolution measurements and to further advance the understanding by making measurements on other light alkali fluorides.

Although the LiF spectrum is very simple compared to the other alkali halides, its features are very broad and we have enhanced the modest changes of slope by various derivative calculations on reflectivity. The study of related compounds was felt to aid in the mutual interpretation of the optical features. Because of the more complicated spectra previously determined in other lithium halides in absorption[2,3] and characteristic energy loss[27] we have worked with sodium fluoride for which there are band calculations[18,28-30] but only fragmentary experimental evidence[5,9,31,32] on the optical constants. In addition, for continuity we have extended the work on KF (Refs. 8 and 33) to lower temperatures and higher resolution.

TABLE I. Theoretical band-to-band energies at the symmetry points in LiF.[a]

	Γ_{15}-Γ_1	L_3-L_2'	X_5'-X_4'	L_3-L_1	X_5'-X_3	X_5'-X_1
PH[b]	13.6	16.4	18.5	20.2	22.4	22.9
P[c]	14.5	17.3	20.5	21.5	22.9	24.4
LS[d]	12.55	15.06	17.97	19.44	21.33	22.38
LS[e]	11.27	13.66	17.07	18.46	20.13	20.79
MLFLC[f]	10.6	12.8	16.8	18.1	19.9	23.5
B[g]	13.6	16.9	18.9			
JAG[h]	13.5	14.8	18.4	19.8	27.7	19.4

[a] Experimental ϵ_2 features: 12.7 p, 13.8 min, 14.7 p, 17.2 p, 20.2 sh, 22.5 p, 28.9 w (p: peak; min: minimum; sh: shoulder; w: weak peak).
[b] Page and Hygh, Ref. 10.
[c] Painter, Ref. 16.
[d] Laramore and Switendick, Ref. 23, solution 1.
[e] Laramore and Switendick, Ref. 23, solution 2.
[f] Menzel *et al.*, Ref. 19.
[g] Brener, Ref. 22.
[h] Jouanin, Albert, and Gout, Ref. 24.

The significant similarities or differences of the spectra of NaF and LiF are the following: The shape of the strong peak near the onset of absorption is very similar, although sharper in NaF. The KF spectrum shows two sharp peaks in this region and these have been interpreted[8,33] as Γ and X excitons. The KF spectrum is further dominated by sharp peaks around 20 eV due to $K^+(3p)$ core levels of an atomic or perhaps excitonic character.[8,33-35] The core levels in NaF and LiF occur beyond the primary region of valence-band excitation, $Na^+(2p)$ and $F^-(2s)$ levels occurring about 33 eV from the conduction band[36-38] and the $Li^+(1s)$ at about 63 eV.[39,40] Recent research on LiF specifically[41-44] and the core absorption problem in general[34,35,45] is leading to a much deeper understanding of the character of the sharp optical excitations originating from core levels in alkali halides. Since the $Na^+(2p)$ levels stand apart so sharply from the other optical features of NaF, and since the $F^-(2s)$ excitation is not evident, we will have little further to say about those core excitations. In LiF our investigations are limited to energies far below the Li core excitation, which appears now to be well understood,[35,42] in any case. The $F^-(2s)$ excitation was not found in LiF but may be the source of a 34-eV feature in KF. For the lighter alkali halides particularly, the optical features are an overlapping composite of excitonic, interband, and perhaps collective excitations. We will not propose many interpretations, but we have noted the existence of differing points of view in the literature. Specifically, we do not find evidence of any intrinsic structure in LiF at energies below 12 eV. The first complete, and in some ranges, the only reflectivity data are presented here for low temperatures of LiF, NaF, and KF as a contribution towards their understanding. We will often have reason to refer to the extremely helpful discussions of Pantelides[35] when describing our data.

First, we will describe the apparatus with which these measurements were made; then we will give the experimental results and discuss them.

II. EXPERIMENTAL TECHNIQUES

Synchrotron radiation from the 240-MeV electron storage ring at the University of Wisconsin

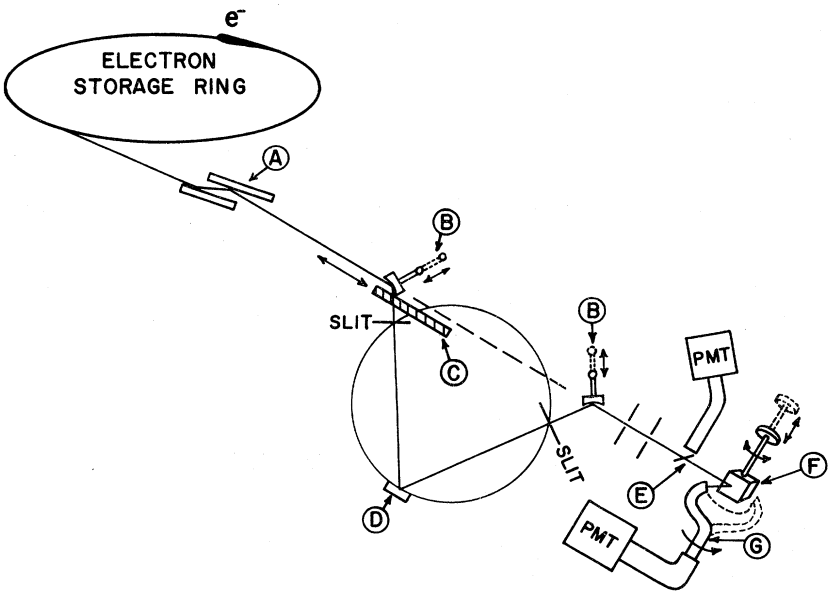

FIG. 1. General experimental arrangement. A: 1:1 focusing mirror system; B: focusing mirror for the monochromator; C: ultraviolet filter holder; D: grating; E: beam splitter; F: sample; and G: rotating light pipe.

Physical Sciences Laboratory[46] was used as a light source in the photon energy range 6–35 eV. Figure 1 is a schematic diagram of the optics of the system. The monochromator, a 1-Seya-Namioka monochromator, was oriented in such a way that the axis of rotation of the grating and the rulings on the grating were parallel to the polarization vector of the light beam. A filter holder was mounted on a bellows-driven linear feedthrough; and aluminum, indium, quartz, MgF_2, and LiF filters were used to eliminate scattered light and higher-order effects of the grating. Figure 2 depicts the inside of the experimental vacuum chamber and attached sample-preparation chamber. The sample could be rotated through 360°. Light in the *p* polarization was reflected off the sample and detected by the sodium-salicylate-coated light pipe and photomultiplier (EMI 9635) combination. The signals from the photomultiplier were preamplified by a photon-counting amplifier[47] and given to a HP 5201L scaler timer. The incident intensity was measured with the light pipe looking directly at the incident light, with the sample moved out of the path of the light pipe by a pneumatically activated double bellows. In the sample-preparation cham-

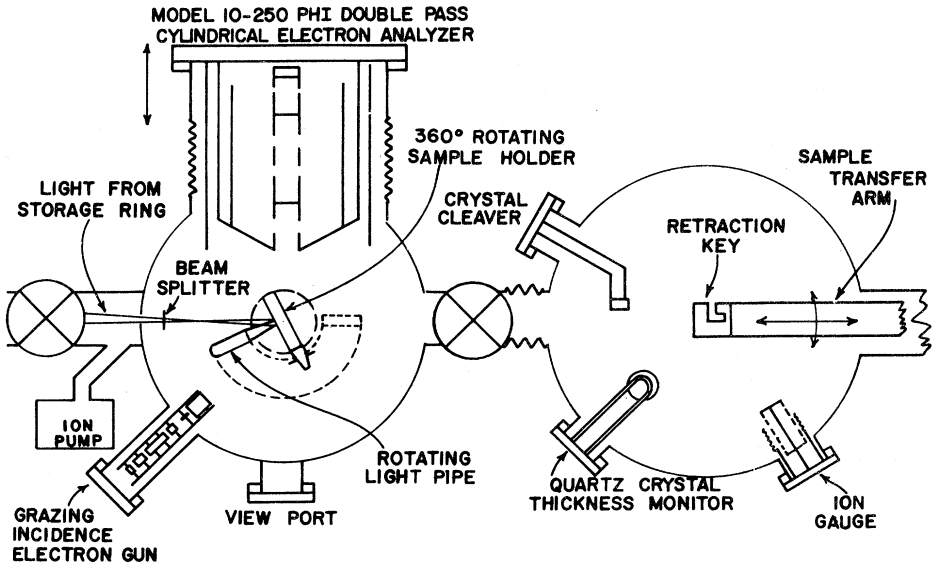

FIG. 2. Details of the sample chamber and sample-preparation chamber.

ber, a lever on a bellows feed-through drove a knife edge for cleaving crystals. The samples were delivered to and picked up from the experimental chamber at high vacuum. The freshly cleaved crystals were exposed to a pressure no greater than 1×10^{-8} Torr for a few seconds, then rested in the low 10^{-9}-Torr range during the reflectivity measurements. The storage ring was maintained by ion pumps at pressures below 10^{-9} Torr. Both the monochromator and the sample chamber were connected to the storage ring without any windows and were pumped out by ion pumps. The monochromator operated at 1×10^{-8} Torr and the sample chamber was operated with differential pumping between the monochromator and the chamber. The sample holder could be cooled by liquid helium, with the sample temperature being determined by a gold-constantan thermocouple attached to the sample holder. The temperature obtained by cooling with liquid nitrogen was about 100 K and the temperature obtained by cooling with liquid helium (Air Products liquid-helium cooling system) was about 30 K at the specimen. Both reflectivity and photoemission measurements could be taken on a sample in this chamber, the details of which are described elsewhere.[48] In these experiments, only reflectivity measurements were made. The data were taken on single crystals purchased from Harshaw Chemicals and cleaved and transferred as described. The average size of the crystal surface on which the data were taken was 1 cm^2 and the typical sample thickness was 3 mm. Extra precautions were taken by making the back surface inclined to the front surface and by roughening the back and side surfaces to eliminate the specular reflections from the back surface in the slightly transparent region near the band edge. The data were taken on LiF at room temperature and 100 K and on NaF and KF at room temperature, 100 and 30 K. We never observed any aging effects, but we did observe different reflectivities which depended on the quality of the particular cleaved surface. Tiny steps or other defects appeared to be the major reason for sample-to-sample differences which were as large as several percent in absolute reflectivity. The quoted reflectivities appear to be most representative of vacuum-cleaved specimens and are based on three or more distinct surfaces.

The whole experiment was interfaced to a PDP-8/E mini-computer and the reflectivity measurements were taken using an interacting FORTRAN program. An extensive set of real-time FORTRAN subroutines containing substantial amounts of assembly language were written to move the monochromator; set the sample, light pipe, and filter positions; gate the scaler-timer for specified time periods and take data from it at the end of gating cycle; read the beam current from the digital voltmeter; and display the data on the x-y recorder. In this particular experiment, the versatile programs took data at constant energy steps, corrected for the background and dead time in the photomultiplier electronics, normalized with beam current, stored data on magnetic tape, and displayed selected information on the x-y recorder. The reflectivity spectrum was obtained by taking the point-by-point ratio of the normalized signal to reference scans. Further details of the computer set-up are described elsewhere.[49] Usable counting rates were obtained in the energy range 40–6 eV. With a 1440-lines/mm, gold-coated 3° 16 sec blazed grating in the monochromator with 40-μm slits and 20-mA storage-ring beam current, peak counting rate in the reference scan was 750,000 counts/sec at about 600 Å. The effects of higher orders in the incident radiation were handled by taking the data with different filters. The slits were adjusted to give adequate counting rates and resolution of 1 Å or better over the entire spectral range. No instrumental broadening effects were observed in our experiments.

Preliminary analysis of the reflectivity data often included averaging, taking the first and second energy derivatives, or taking temperature derivatives. For the latter we used reflectivity data files taken at two different temperatures and calculated the logarithmic temperature derivative. Finally, the reflectivity data were Kramers-Kronig (KK) analyzed using the method of Veal and Paulikas.[50] Details of all the above programs are described elsewhere[49] and are available on request.

III. EXPERIMENTAL RESULTS

All figures of experimental reflectivity in this paper are unretouched computer-output graphs of reflectivity files, so they contain no interpretive manipulation. Figure 3 shows the normal incidence (9°) reflectivity of LiF at 100 K and Fig. 4 shows a calculated ϵ_2. The experimental data from 12 to 30 eV were used for the analysis. In the KK analysis, data for LiF below 12 eV were calculated using a model harmonic oscillator because the measured values from 6 to 12 eV could have been subject to artifacts such as F-center phenomena arising from the transparency of LiF in that region. There were no significant variations between measured and calculated reflectivities, however, and there was no evidence of any structure between 6 and 12 eV which might have been associated with bulk band-structure effects. The parameters for the calculated oscil-

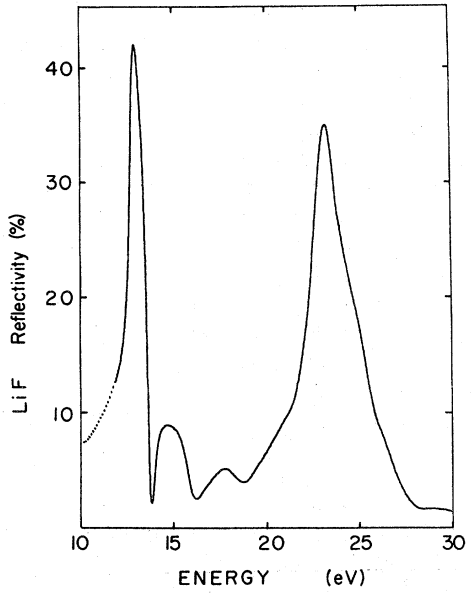

FIG. 3. Near-normal-incidence reflectivity of LiF at 100 K.

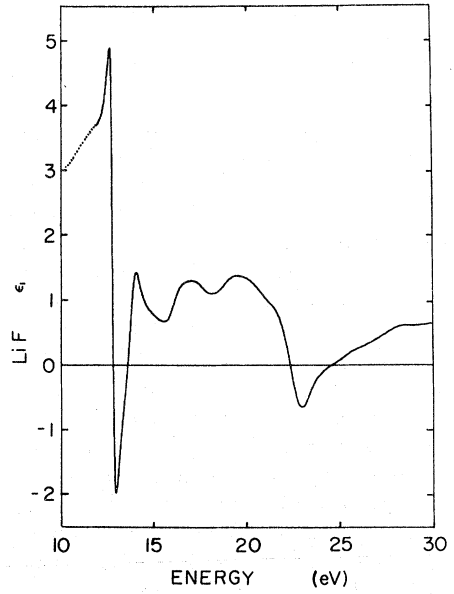

FIG. 5. Real part of the dielectric function (ϵ_1) of LiF at 100 K.

lator were chosen to match the reflectivity and its slope at 12 eV and the refractive index in the visible region. The shape of computed features below 12 eV depends strongly on the specific extrapolation used.

The extrapolation to high energy has much greater uncertainty and influence on the magnitudes of dielectric constants.[50] KK analyses were made with a large number of extrapolations. Evidence pointing towards the most suitable extrapolation is found by monitoring ϵ_2 magnitude at low energy where it should be positive and approaching zero near 10 eV, examining the several sum-rule integrals, and looking for regions of unphysical computed phase, for example. Since the resulting dielectric function calculation is a compromise, the

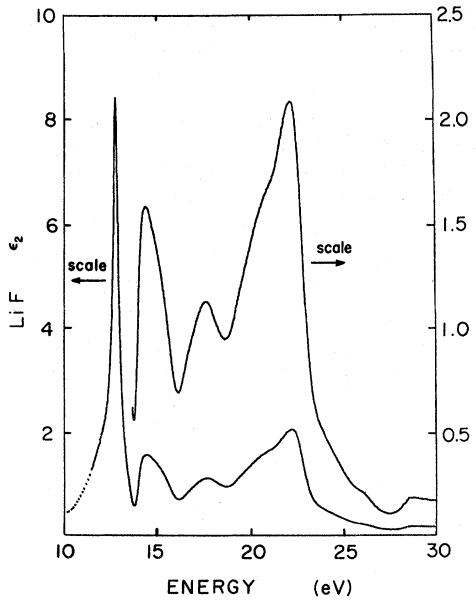

FIG. 4. Imaginary part of the dielectric function (ϵ_2) of LiF at 100 K.

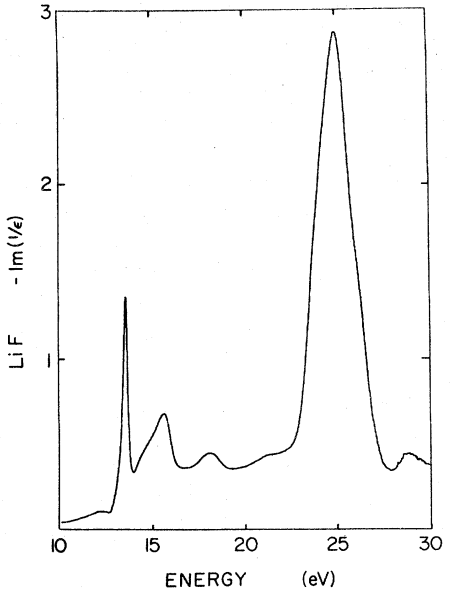

FIG. 6. Dielectric loss function $-\mathrm{Im}(1/\epsilon)$ of LiF at 100 K.

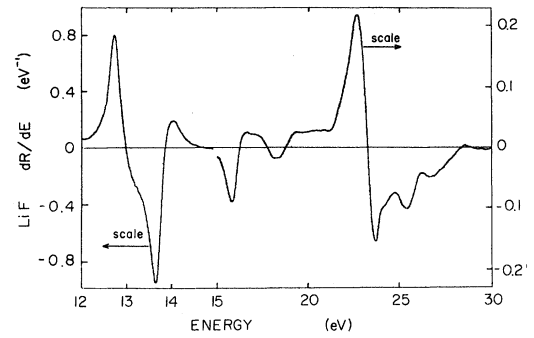

FIG. 7. First energy derivative of the reflectivity of LiF at 100 K. Note the change in both the horizontal and vertical scales.

magnitudes are uncertain to 15% typically. No new structure is introduced within the range of the experimental data by the extrapolation. On the other hand, all sum-rule integrals and computation of effective numbers of contributing electrons vary markedly with extrapolation details and will not be discussed further in what follows.

Since the light pipe could be directed away from the specular beam, it was easy to show that the effect of any fluorescence was negligible. The data were obtained in steps of 0.01 eV and the dielectric constants were calculated for that interval, thus permitting interesting derivatives to be taken of the optical constants. Figures 5 and 6 show the calculated ϵ_1 and $\epsilon_{\text{loss}} = -\text{Im}(1/\epsilon)$. Figures 7 and 8 show the first and second energy derivatives of the reflectivity at 100 K. All derivatives are computer calculations using smoothing as required. Note that there are differences in both the x and y scales for different ranges in the figures. The temperature-difference spectrum between room-temperature and 100 K data resembles the first derivative of the reflectivity versus energy spectrum, since the primary temperature effect is to displace the spectrum smoothly in energy, although differential energy changes and sharpening give some clues to the origin of spectral features. The logarithmic temperature derivative in the range 12–30 eV is shown in Fig. 9.

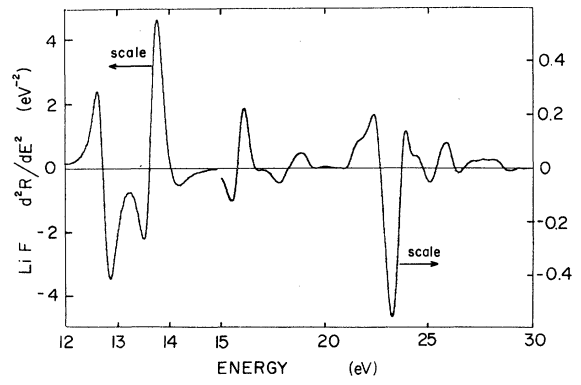

FIG. 8. Second energy derivative of the reflectivity of LiF at 100 K. Note the change in both the horizontal and vertical scales.

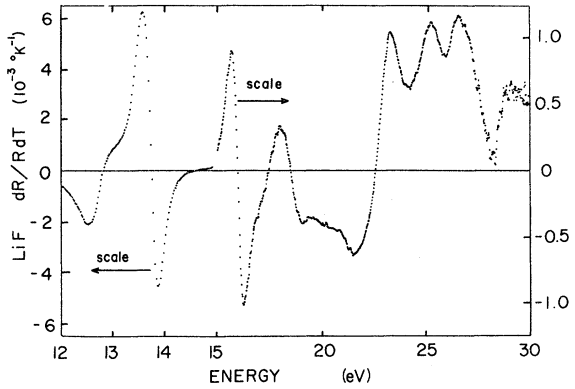

FIG. 9. Logarithmic temperature derivative of the reflectivity of LiF, calculated from the data at 100 and 300 K.

The spectrum is in substantial agreement with RW, but since we also performed low-temperature experiments on a number of specimens, we are able to point out additional structure, particularly in the higher-energy ranges. Peak positions of all prominent peaks in R, ϵ_2, and ϵ_{loss} together with the experimental data on energy loss by Creuzburg[27] and the temperature coefficients for reflectivity data are given in Table II. Also indicated is the structure in the high-energy part

TABLE II. Peak positions in LiF in eV at 100 K. Temperature coefficients were computed by 300–100-K differences in reflectivity.

R	ϵ_2	ϵ_{loss}	Temperature coefficient (-10^{-4}eV/°K)
12.98 p	12.7	13.7 (13.5) [a]	8.3
13.6 sh	13.6		
14.6 p	14.2	15.7 (15.5)	6.2
	15.2		
16.8	16.7	18.1 (18.1)	10.6
17.7	17.6		
~20 sh	20.2±0.5 sh	21.2	
23.25 p	22.5	25.1 (25.3)	6.7
~25.1 sh	24.8		
~26.4 sh	26.2		
~28.9 w	28.9±0.5	28.8 (29.6)	

[a] Creuzburg's (Ref. 27) experimental data in parentheses.

of the 23-eV peak. Peak positions were determined from the energy derivatives in general, which aid in roughly locating the shoulder positions.

The main peak at 12.98 eV is highly asymmetric as noted earlier by RW and is developed in the derivative spectra. Both 14.6- and 17.7-eV lines in the reflectivity may conceal additional structure as inferred from the second derivatives of R and ϵ_2, but in seven or eight specimens we never observed the distinct doublet reported by Stephan in the 17.7-eV peak. The strong shoulder at 20 eV is quite complex, as seen in Fig. 9, for example. The calculated energy loss is in very good agreement with actual measurements of Creuzburg[27] and, more recently, by Gibbons *et al.*[51] We cannot explain why our ϵ_{loss} at the 25-eV peak is about three times larger than observed[27] but we will have more to say on this below. The structures in the 23-eV peak are of uncertain origin and have not been reported previously, although absorption studies by Saito *et al.*[32] point towards a complicated structure. They are easily seen in low-temperature data and, of course, in all derivatives, but are much less evident in room-temperature data. The weak reflectivity peak at 28.9 eV (28.9 in ϵ_2) is also reported here for the first time, although a loss peak near 29.6 eV was previously reported.[27] We observed no structure in the reflectivity from 30 to 35 eV above the considerable noise due to the small intensity and reflectivity in that range. Transitions from the $F^-(2s)$ core levels were not observed. Several arguments have been advanced by Pantelides[35] for failure to observe halogen ion-core excitations.

Figure 10 shows the normal incidence reflectivity of NaF at 30 K in the range 6–30 eV. The data were taken without any filter in the range 30–12 eV and with a LiF filter in the range 12–6 eV. The peak at 10.5 eV has the highest reflectivity of all three substances studied here. The reflectivities are very small beyond 12 eV, but long counting times were not required, since the incident intensity from the electron storage ring was very high in this region for the selected grating. Figure 11 shows the calculated ϵ_2 from the experimental R data at 30 K in the range 9–30 eV. Figure 12 shows ϵ_1 and Fig. 13 shows the ϵ_{loss} function. The details of the extrapolation critically affect the magnitude of the calculated dielectric function, similar to the case for LiF.

The main peak at 10.5 eV in R is highly asymmetric, as described earlier by RW and Saito *et al.*[32] and a splitting is clearly resolved in the derivatives. The position of the shoulder in the high-energy side of the peak is 0.43 eV from the main peak. This is very weak in ϵ_2 and cannot be easily identified even in the derivatives of ϵ_2, as we did for LiF. The two broad peaks at 16 eV remained roughly the same as the sample was cooled, but the peak at 20.5 eV sharpened and split into two parts. Although they are not very well resolved in ϵ_2, the two peaks can be seen in the first energy derivative which is shown in Fig.

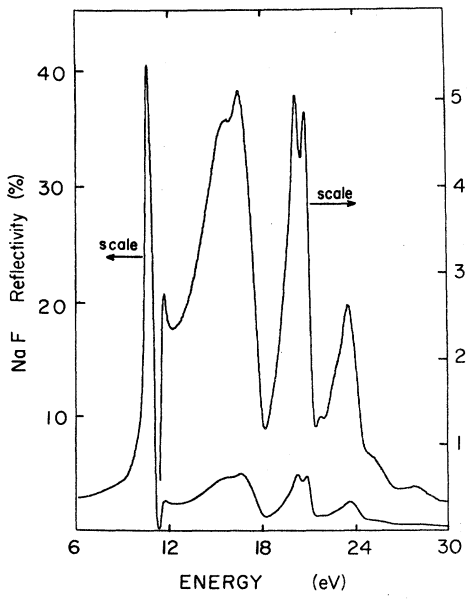

FIG. 10. Near-normal-incidence reflectivity of NaF at 30 K.

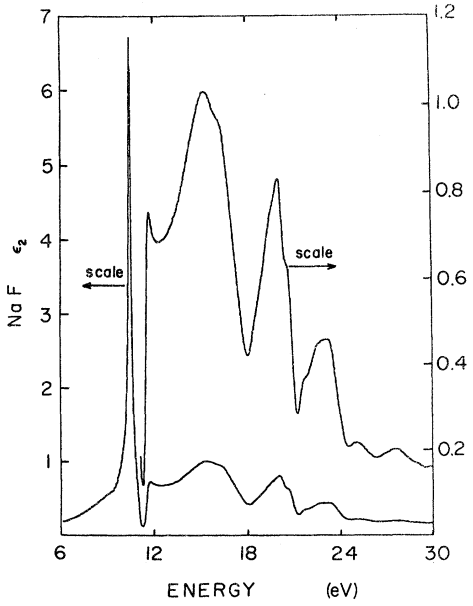

FIG. 11. Imaginary part of the dielectric function (ϵ_2) of NaF at 30 K.

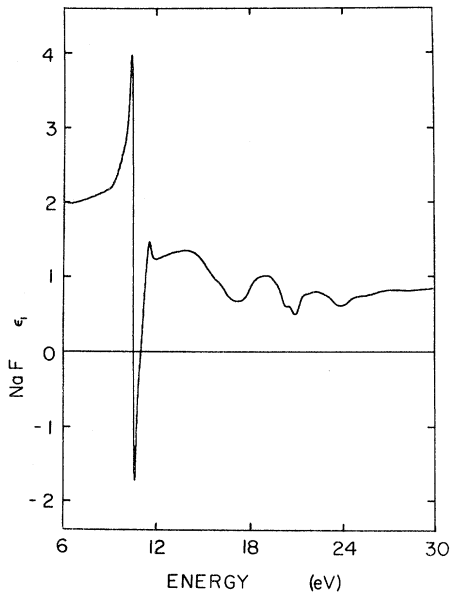

FIG. 12. Real part of the dielectric function (ϵ_2) of NaF at 30 K.

14. The small sharp peak at 21.72 eV is seen only at low temperature, as is the shoulder at 22.67 eV. The spectrum contains two broad peaks beyond the main peak at 23.62 eV at 26.4 and 28.1 eV. This part of the spectrum is very similar to the LiF spectrum, although considerably weaker.

Since the $Na^+(2p)$ absorption occurs at 33 eV, the

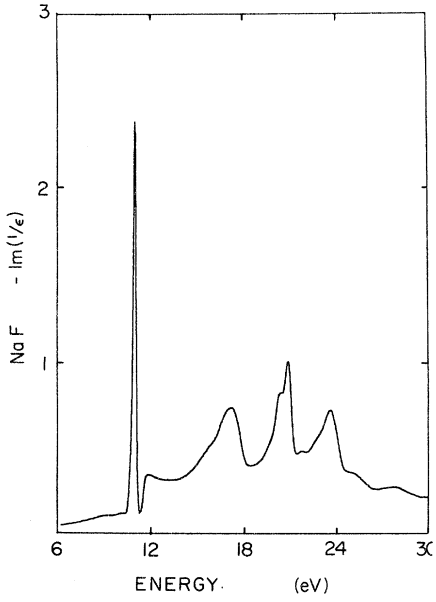

FIG. 13. Dielectric loss function $-\mathrm{Im}(1/\epsilon)$ of NaF at 30 K.

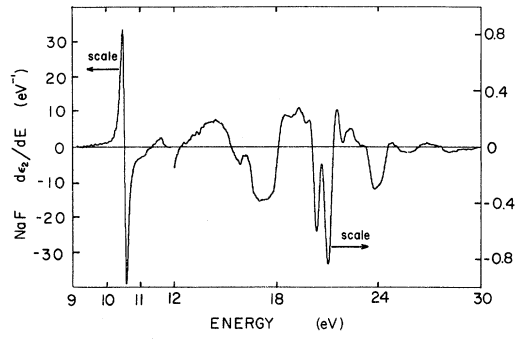

FIG. 14. First energy derivative of ϵ_2 of NaF at 30 K. Note the changes in both the vertical and horizontal scales.

reflectivity studies were extended to 35 eV. A broad and small (1%) peak at 31.45 eV and the sharp $Na^+(3p)$ core exciton at 33.14 eV were observed. The position and structure of the sharp peak is in substantial agreement with the core-exciton absorption data.[36-38] The peak reflectivity of the sharp doublet is about 3%.[49] This peak is not further analyzed here, since its identification and structure are well established and our data quality became poor at energies corresponding to the assumed core-conduction band gap near 35 eV. The two peaks at 31.4 and 28.1 eV are in good agreement with the only absorption measurement in that range.[38] The quoted values in the absorption are 31.3 and 27.6 eV. Table III gives the peak and shoulder positions of the 30 K R, ϵ_2, and ϵ_{loss} data together with Creuzburg's[27] experimental energy-loss data. The temperature coefficients

TABLE III. Peak positions in NaF in eV at 30 K. Temperature coefficients were computed from 300–100-K differences in reflectivity.

R	ϵ_2	ϵ_{loss}	Temperature coefficient (-10^{-4}eV/K)
10.66 p	10.55	11.1 (10.9)[a]	7.5
11.77 w	11.77	11.9 (11.9)	
15.72 p	15.3	15.8 (17.4)	0.9
16.57 p	16.5	17.4	
20.26	20.1	20.4 (20.8)	3.0
20.89	20.8	21.0	
21.72 p	21.6	21.8	
22.67 sh	22.5	22.8	
23.62 p	23.4	23.8 (23.7)	6.0
26.37 w	25.1	25.3	
28.08 w	27.8	28.7	
31.45 w			
33.14 p		(33.2)	

[a] Creuzburg's (Ref. 27) experimental data in parentheses.

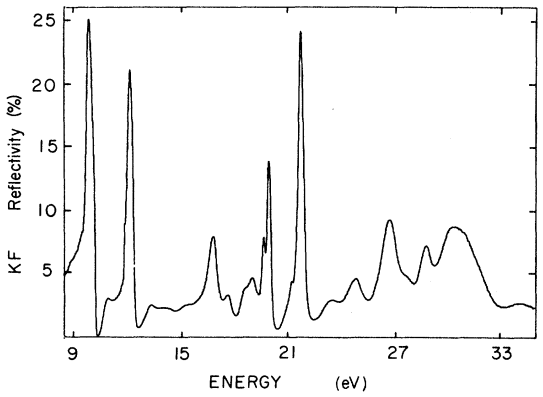

FIG. 15. Near-normal-incidence reflectivity of KF at 30 K.

for the motion of the strong peaks are also given in Table III.

Potassium fluoride is the third member of the series we studied. It is very hygroscopic and the reflectivity of crystals cleaved in air did not correspond well to the reflectivity of crystals cleaved in vacuum. The difference is dramatic in this case. The present results were taken with the crystals cleaved and maintained in vacuum. Figure 15 shows the reflectivity at 30 K with 0.01-eV spacing. This is the combined reflectivity spectrum taken with different filters. The data between 17 and 11 eV were taken with an indium filter, and the data between 12 and 9 eV were taken with a LiF filter. The spectrum is in fair agreement with the data reported by previous investigators and a host of new features are either observed or confirmed with higher resolution. The data are of high resolution and the magnitude of the reflectivities at the peaks are quite a bit higher than those of previous investigations. Cleaving the crystal in vacuum, using a high-resolution monochromator, the continuous nature of the synchrotron radiation, and the ability to cool the sample to low temperatures contributed to the character of the reflectivity spectra reported here. The relative energy splittings can be measured to an accuracy of 0.01 eV. The absolute energies were also measured to the same accuracy by calibration with mercury vapor lines.

The reflectivity in the range 23–35 eV shows five sharp peaks and a small broad peak at 23.39, 24.8, 26.7, 28.8, 30.3, and 34.2 eV, respectively. There are two shoulders on both wings of the 26.7 line. The shoulder on the high-energy side is very clearly seen in the reflectivity at 27.8 eV. The shoulder on the low-energy side at 25.9 eV is very difficult to see in the reflectivity, but can be seen in the first and second derivatives. These features were not observed or only poorly seen in earlier reports.[8,33] The magnitude of the reflectivity beyond 30 eV should be taken with caution, since corrections for scattered light are very important and are not made for the data illustrated. We do not expect any changes in the structure because of this limitation. Editing of the data at high energies for purposes of extrapolation in the KK program illustrated the scale of uncertainties generated by magnitude errors in the reflectivity. We discussed these uncertainties above in reference to LiF.

The reflectivity in the range 19–23 eV is dominated by excitations from the $K^+(3p)$ core. The two strong peaks at 21.79 and 20.00 eV have been assigned[33] to X and Γ excitons, but Pantelides[35] has urged caution in relating excitons to specific critical points. The Γ exciton is split into two, perhaps because of the spin-orbit interaction, and the second component which is on the low-energy side of the 20.00-eV peak can be seen only as a shoulder in the room-temperature data, but appears as a strong narrow peak in the low-temperature data. The peak at 21.79 eV has the highest reflectivity in this region of the spectrum, with a value comparable to that of the valence-band excitons. There is evidence of a strong shoulder in the low-energy part of this peak in the room temperature data, but this is sharpened into a narrow, fairly strong peak at low temperature. This is too far below the X exciton to be a spin-orbit split component of it. From a comparison to other potassium halides, this might be assigned to the A_1' excited state of the exciton,[7] but again the remarks of Pantelides[35] should be noted. This was seen previously in the reflectivity and absorption studies of KF as a shoulder. In the region between 18 and 20 eV there is a broad peak in the room-temperature data at 18.67 eV, but this is clearly split into two parts in the low-temperature data, the peaks occurring at 18.7 and 19.0 eV.

The region 13–19 eV includes mainly the transitions coming from the valence band to the higher-conduction bands. Two strong narrow peaks at 17.65 and 16.88 eV and two rather broad peaks at 15.3 and 14.1 can be seen in this range. These features were not resolved in the previously published data.

The region 8–13 eV is dominated by valence-band excitons. The strong peak at 12.23 may be due to the X exciton, and that at 10.4 eV may be due to the Γ exciton. The 10.4-eV peak is highly asymmetric and showed splitting in the energy derivatives similar to the LiF and NaF data. The value of the reflectivity at the dip in the lowest-temperature data is remarkably close to zero.

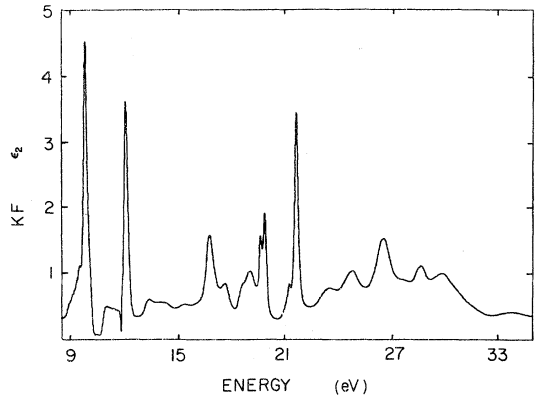

FIG. 16. Imaginary part of the dielectric function (ϵ_2) of KF at 30 K.

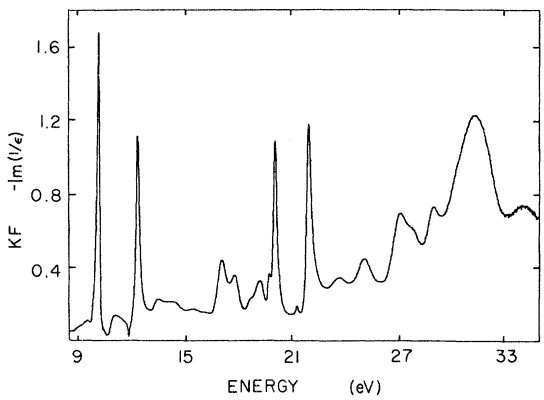

FIG. 18. Dielectric loss function $-\mathrm{Im}(1/\epsilon)$ of KF at 30 K.

The value is 0.01% with some uncertainty due to background correction problems. The line shape of the assumed X exciton did not show as much asymmetry as the Γ exciton, and the first and second energy derivatives support the identification as a single resonance peak. Considerable structure of uncertain origin appears (by cooling to 100 K or below) in the low-energy tail of the Γ exciton. It is not a fluorescence effect, nor has it been reported in more detailed[3,52] investigations of these lower-energy features. We will not discuss this further at the present time.

Fig. 16 shows the calculated ϵ_2 for the low-temperature data, and Figs. 17 and 18 show the calculated ϵ_1 and ϵ_{loss} functions. The peak positions in R, ϵ_2, and ϵ_{loss}, the experimental energy-loss function, and the temperature coefficients for the strong peaks are given in Table IV.

The data were taken at discrete energies, and the variation of reflectivity with temperature is illustrated in Fig. 19 in the $K^+(3p)$ excitation region. In this region, instrumental broadening may become significant and higher-resolution studies could be fruitful. Figure 19 is particularly revealing, showing the improvement in resolution and the very different thermal shifts of the 20- and 22-eV peaks.

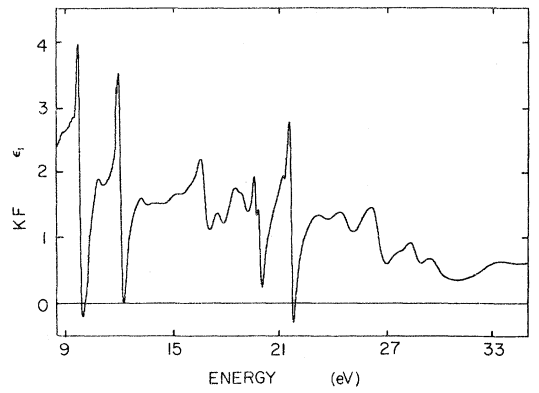

FIG. 17. Real part of the dielectric function (ϵ_1) of KF at 30 K.

TABLE IV. Peak positions in KF in eV at 30 K. Temperature coefficients were computed from 300–100-K differences in reflectivity.

R	ϵ_2	ϵ_{loss}	Temperature coefficient (-10^{-4}eV/K)
9.98 p	9.88	10.23 (10.00)	11.0
12.23 p	12.13	12.43 (12.40)	3.0
13.33 w	13.43	13.5	
14.06 w	13.98	14.1 (13.6)	
15.32 w	15.48	15.5	
16.88 p	16.88	17.13 (17.25)	
17.65 p	17.68	17.73	
18.7 p	18.8	18.8 (18.85)	
19.0 p	19.08	19.13	
19.7 w	19.68	19.78 (20.15)	4.5
20.0 p	19.93	20.13	
21.29 w	21.3	21.33	
21.79 p	21.73	21.98 (22.05)	0.5
23.39 p	23.48	23.63 (23.3)	
24.83 p	24.83	25.08 (25.1)	
26.74 p	26.58	27.13 (27.6)	4.7
27.8 sh	27.7 sh		
28.8 p	28.68	29.03 (28.8)	
30.35 p	29.83	31.13 (31.3)	−5.0
34.22 p	33.78	34.2 (34.3)	

[a] Creuzburg's (Ref. 27) experimental data in parentheses.

IV. DISCUSSION

In this section we would like to summarize what we have accomplished experimentally. While trying to avoid excessive speculation, we will attempt to interpret several spectral features appearing in all three compounds within the framework of existing band-structure calculations and the corresponding atomic viewpoint. The reflectivity spectra of LiF and NaF are somewhat similar and our work on these compounds is summarized first; the summary of KF is given later.

Reliable one-electron band-structure calculations have been quite successful in explaining a host of physical properties of materials where the transition energy is a few eV or less. Optical and electrical properties of semiconductors and metals in the infrared and visible spectral regions are some examples of the success of the theory. Realistic one-electron band-structure calculations of large-gap insulators have become available only in the last decade and the ultraviolet and soft-x-ray properties of solids have become clarified only during the last couple of years. The interpretation of the ultraviolet and soft-x-ray spectra of solids is somewhere between atomic spectroscopy, where electrons retain their atomic configuration and semiconductor physics, where the interband effects play the dominant role. The applicability of these two viewpoints, namely the band versus the atomic points of view, is the subject of current interest.[35,53] Since transitions from flat core states do not appear[35] to give a simple representation of conduction-band density of states in alkali halides, it is difficult to use interband transitions from the valence band to give critical point separations.

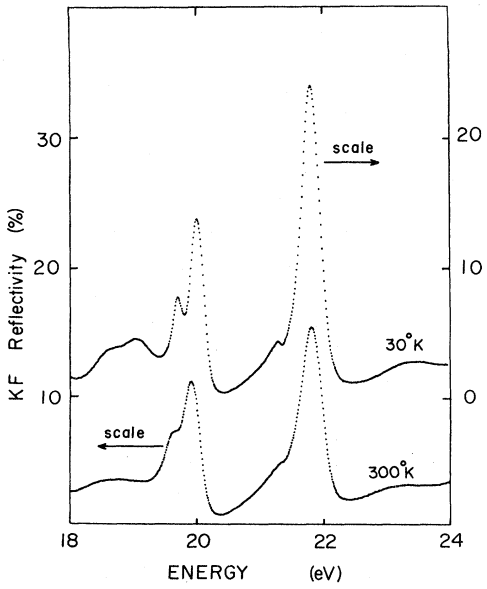

FIG. 19. Near-normal-incidence reflectivity of KF at 300 and 30 K in the range 18–24 eV.

First, we will discuss the 12.7-eV peak in the case of LiF. If the band gap were around 11 eV and the strong peak at 12.7 were a transition due to a broad region near the L point, there would be difficulties in accounting for the high transparency of LiF to 12 eV, the absence of excitons, and the small implied energy difference at the L or X point in the Brillouin Zone (BZ) compared to the band gap. This difference is more than a few eV for any realistic band-structure calculation, since the valence band has a width of several eV and the conduction band is more like a free-electron band rising several eV from Γ to L or X. We cannot match the gaps at Γ and L points and the transparency in any consistent way in the above model. The small discontinuity seen at 12 eV in ϵ_{loss} is an effect of the extrapolation procedure in the KK analysis.

In the excitonic interpretation, one takes the band gap to be around 13.6 eV and explains the strong peak at 12.7 eV as the Γ exciton[5] and other features in that range as due to higher exciton states, excitons at different locations in the zone, and crystal symmetry splittings.[11] The case for the interpretation of the strong peak near the absorption threshold of NaF is the same as the above, but our study did not give any more insights into the interpretation. It is clear that far greater resolution would be required before a useful statement could be made relating to the many possible splittings. A dynamic-modulation study like electric-field modulation or temperature modulation should help in identification, compared to the energy derivatives and the temperature-difference spectra we have obtained in this work. We did not anticipate that a study of LiCl or LiBr would help in the interpretation because of the added complexity of the sizable spin-orbit splitting. The spectra of heavy alkali halides are all quite dissimilar to those of LiF and NaF.

The rest of the interpretation is carried out on the basis of the exciton model. There is no specific signature of the transition at the Γ point above the sharp peak except for the sharp rise in reflectivity near 13.6 eV. Taking 13.6 eV as the bank gap,[5] the exciton binding energy is about 1 eV if explicitly associated with a critical point at Γ. Additional structure at 14.4 eV with complexities inferred from the second derivative of ϵ_2 cannot correspond to transitions at the L region of the BZ because of the conflict mentioned previously. The separation of L must be several eV larger than the separation at Γ. A plausible explanation

is that these complexities are due to higher exciton states and excitons at different locations in the zone. The line at 17.7 also conceals additional structure, as inferred from the second derivative of ϵ_2, and this is the most likely region for the interband transitions at the L point in the zone. The splitting as observed in the second derivative is 0.9 eV, which is of the same order as the splitting observed in the valence-band density of states in the x-ray photoemission (XPS) experiment.[54] This peak might be due to a combined effect of transitions from valence to conduction band, including the effects at L and X points, and a few low-lying higher conduction bands. There is no specific signature of such BZ points, and the wide variety of theoretical band-structure calculations prevents a secure interpretation. The spectrum of NaF is markedly different from that of LiF in this region and is of little help in clarification.

The NaF spectrum shows a very clear doublet at 16 eV and a very sharp and clear doublet at 20 eV. The origin of the 16-eV doublet is probably from transitions at the L region. The band-structure calculation of Brener[28] gives the band gaps $L_3' - L_2'$ as 17.0, $L_3' - L_1$ (higher conduction band) as 17.2 and $X_5' - X_4'$ as 18.1 eV. The splitting in our observed spectrum is 1.2 eV and might correspond to the separation of the two branches in the BZ at the L point. From the $Na^+(2p)$ core interpretation,[36b] a Γ-X separation of about 6 eV in the conduction band could be supported with great uncertainty. The above-mentioned caution should be taken again in the assignment. The doublet at 20 eV shows a very clear splitting at low temperature, and might be assigned to valence-band-to-higher-conduction-band transitions at the X point ($X_5' - X_1$ is calculated[28] to be 20.0 eV). The splitting of 0.7 eV might correspond to the separation of the two branches of the valence band at the X point. In LiF, from comparison with the NaF result, the shoulder at 20 eV with its complicated structure might correspond to the above transitions at the X point.

The reflectivity peak in LiF at 23.25 eV has been widely discussed. Referring to the associated peak in ϵ_2 at 22.5 eV, Kunz and co-workers[11,25] identify this as a scattering state of the electronic polaron. It will be noted from Fig. 4 that the weak reflectivity shoulder has become a strong feature in ϵ_2 at about 20 eV. It is probable that many interband critical points lie in this energy range as well. The complex but weak structures on the high-energy side of the 22-eV peak lie at energies appropriate to excitation of two excitons[26] or bound and free electronic polarons[25] but there is as yet no firm experimental or theoretical basis for identifying the weak features at 24.8, 26.2, and 28.9 eV. The zero crossing of ϵ_1 near 25 eV generates a very large computed value of ϵ_{loss}. This peak has been associated with plasmon excitation[5,26] corresponding to a large experimental electron energy-loss peak.[27,51] We calculate a weak ϵ_{loss} peak at 21.2 eV, where an independent-loss experiment has resolved a similar weak peak.[51] The main envelope of the large-loss peak at 25 eV probably covers the combined phenomena mentioned above including collective excitations and interband excitations.

The explanations of the high-energy features of NaF up to 33 eV also remain quite uncertain. The general features are similar to the case of LiF, although the ϵ_{loss} peak is greatly reduced in intensity. The description of these peaks again may include a combination of collective excitations and valence-band–to–higher-conduction-band transitions, but we have no specific evidence on these points.

Optical transitions from the $F^-(2s)$ level to the conduction band, which occur at about 34 eV in LiF (Ref. 55) are forbidden in the atomic model and expected to be very weak in the solid.[35] We looked for any structure in the reflectivity in the range 30–35 eV, but did not find any above the considerable noise in that energy range. The sharp peak observed at 33.1 eV in the $Na^+(2p)$ spectrum is described as excitonic, with a band threshold at 36.3 eV and a binding energy of 3.2 eV.[35] The band threshold for the $F^-(2s)$ spectrum lies 1.5 eV below the band threshold[35] of $Na^+(2p)$, and some of the structure in the range 25–32 eV might be due to it, but we cannot give any positive identification. In NaF the sharp and tiny peak at 22 eV in reflectivity is exceptional, lying on a broad continuum far from expected atomic or excitonic effects. We propose no interpretation.

The reflectivity and dielectric-function data of KF are shown in Figs. 15–18, and the peak positions are given in Table IV. The reflectivity spectrum of KF is markedly different from those of LiF and NaF, and is generally similar to the reflectivity of other alkali halides.[7] The main features near the absorption threshold are identified as Γ and X excitons,[8,33] and the additional structure in these peaks is discussed elsewhere. The three weak peaks in the range 13–15 eV are presumably due to interband transitions. The two strong peaks illustrated in Figs. 19 at 20 and 22 eV have been identified as Γ and X core excitons[8,33] with a small (1.5 eV) binding energy. Both of these are resolved as doublets in our data. An alternative description of such sharp transitions by Pantelides[35] rests on a more complete analysis. He puts the band threshold at 23.9 eV and identifies all nearby sharp structure at lower energies with

excitonic character and binding electron-hole interaction, the hole at the K^+ ion not being effectively screened. Instead of assigning the transitions to excitons at specific critical points, he notes the evidence for large mixing of band states over energy ranges of many eV. Transitions near 20 eV are assigned to $K^+(3p\text{-}4s)$ transitions and those near 22 eV may be $K^+(3p\text{-}4d)$ transitions.[35] Figure 19 shows how the shoulder at 21 eV, interpreted as a band edge,[33] becomes much more complex upon cooling. It is interesting that the 22-eV peak, unlike that at 20 eV, scarcely shifts upon cooling. Although some evidence on relative core-level shifts with temperature is available,[56] data are incomplete on this point for KF.

The spectrum beyond 25 eV remains rich in interband-like transitions, but we are not able to make a confident interpretation of individual features. Although the $F^-(2s)$ excitation has been placed at 29 eV,[55] it probably occurs at about 33 eV,[54a] as discussed by Pantelides.[35] The broad hump at 34 eV in reflectivity (33.5 eV in ϵ_2) is well isolated from the other, sharper features in that energy range. If this feature is due to a $F^-(2s)$ transition it would be interesting evidence relating to transition probabilities and lifetimes of halogen-ion core transitions.[35]

We will conclude with some remarks on the comparison of our computed values of $-\mathrm{Im}(1/\epsilon)$ and the energy-loss data of Creuzburg.[27] In all three substances the relative magnitudes, and particularly the positions of loss features, are in excellent agreement except for two considerations. The magnitude of the very sharp features is much smaller in Creuzburg's work, presumably because of instrumental broadening in his measurements. Our low-temperature results, in particular, point to a large number of additional features, all of which may be found as shoulders or plateaus in the direct loss measurements. The second problem is that whereas the absolute magnitude of ϵ_{loss} is in quite reasonable accord in the two experiments for NaF and KF, being within about 30% of each other, the magnitude for LiF is substantially different. This disagreement was also noted and discussed by RW who found as we did that the computed ϵ_{loss} was about three times as large as observed. Since the difference in magnitude was not observed for NaF and KF, we cannot point to any systematic problem. The relative scale and detailed shape of the energy loss measured for LiF in recent work[51] are in very close accord with our conclusions, but no absolute scale is yet available for the recent work so it is not yet clear if a definite difference exists. In any case, while the agreement is comforting, it is not evident how to improve any interpretation of the optical features by further discussion of the comparison of our data and the energy-loss experiments.

ACKNOWLEDGMENTS

We wish to thank E. Rowe, R. Otte and C. H. Pruett of the Synchrotron Radiation Laboratory for their many kindnesses and John Steben and Robert Bennett for their assistance in programming and interfacing the computer. We are also grateful to Boyd Veal for helping us to develop his Kramers-Kronig analytic methods in a form suitable for alkali halides. We have also profited from the general advice on vacuum ultraviolet techniques from C. Olson and U. S. Whang. The electron storage ring at the time of this research was supported by the Air Force Office of Scientific Research under Research Grant No. AFOSR-F44620-70-0029.

---

†Supported by the Air Force Office of Scientific Research under Grant No. AFOSR-70-1906 with additional support by the Wisconsin Alumni Research Foundation.

[1]R. Hilsch and R. Pohl, Z. Phys. 59, 812 (1930).
[2]J. E. Eby, K. Teegarden, and D. B. Dutton, Phys. Rev. 116, 1099 (1959).
[3]K. Teegarden and G. Baldini, Phys. Rev. 155, 896 (1967).
[4]G. Baldini and B. Bosacchi, Phys. Rev. 166, 863 (1968).
[5]D. M. Roessler and W. C. Walker, J. Phys. Chem. Solids 28, 1507 (1967).
[6]D. Blechschmidt, R. Klucker, and M. Skibowski, Phys. Status Solidi 36, 625 (1969).
[7]G. W. Rubloff, Phys. Rev. B 5, 662 (1972).
[8]G. Stephan and S. Robin, C. R. Acad. Sci. (Paris) 267, 1286 (1968); D. M. Roessler and H. J. Lempka, Br. J. Appl. Phys. 17, 1553 (1966).
[9]D. M. Roessler, Ph.D. thesis (University of London, 1966) (unpublished).
[10]L. J. Page and E. H. Hygh, Phys. Rev. B 1, 3472 (1970).
[11]D. J. Mickish, A. B. Kunz, and T. C. Collins, Phys. Rev. B 9, 4461 (1974); T. C. Collins, A. B. Kunz, and J. T. DeVreese, Int. J. Quantum Chem. Symp. 7, 551 (1973).
[12]G. Stephan, thesis (University of Rennes, France, 1970) (unpublished).
[13]D. H. Ewing and F. Seitz, Phys. Rev. 50, 760 (1936).
[14]A. B. Kunz, T. Miyakawa, and S. Oyama, Phys. Status Solidi 34, 581 (1969).
[15]R. C. Chaney, E. E. Lafon, and C. C. Lin, Phys. Rev. B 4, 2734 (1971).
[16]G. S. Painter, Int. J. Quantum Chem. 5, 501 (1971).
[17]D. M. Drost and J. L. Fry, Phys. Rev. B 5, 684 (1972).

[18]F. Perrot, Phys. Status Solidi B 52, 163 (1972).
[19]W. P. Menzel, C. C. Lin, D. F. Fouquet, E. E. Lafon, and R. C. Chaney, Phys. Rev. Lett. 30, 1313 (1973).
[20]A. B. Kunz, D. J. Mickish, and T. C. Collins, Phys. Rev. Lett. 31, 756 (1973).
[21]D. J. Mickish and A. B. Kunz, J. Phys. C 6, 1723 (1973).
[22]N. E. Brener, Phys. Rev. B 7, 1721 (1973).
[23]G. E. Laramore and A. C. Switendick, Phys. Rev. B 7, 3615 (1973).
[24]C. Jouanin, J. P. Albert, and C. Gout, C. R. Acad. Sci. B. 278, 743 (1974).
[25]J. T. DeVreese, A. B. Kunz, and T. C. Collins, Solid State Commun. 11, 673 (1972).
[26]T. Miyakawa, J. Phys. Soc. Jpn. 17, 1898 (1962); 24, 768 (1968).
[27]M. Creuzburg, Z. Phys. 196, 433 (1966).
[28]N. E. Brener and J. L. Fry, Phys. Rev. B 6, 4016 (1972).
[29]N. E. Brener, Int. J. Quantum Chem. Symp. 7, 559 (1973).
[30]A. B. Kunz, T. Miyakawa, and W. B. Fowler, Mem. Soc. R. Sci. Liege 20, 263 (1970).
[31]R. Sano, J. Phys. Soc. Jpn. 27, 695 (1969).
[32]H. Saito, S. Saito, and R. Onaka, J. Phys. Soc. Jpn. 28, 699 (1970).
[33]D. Blechschmidt, R. Haensel, E. E. Koch, V. Nielsen, and M. Skibowski, Phys. Status Solidi B 44, 787 (1971).
[34]C. Satoko, Solid State Commun. 13, 1851 (1973).
[35]S. T. Pantelides, Phys. Rev. B 11, 2391 (1975).
[36](a) S. Nakai, T. Ishii, and T. Sagawa, J. Phys. Soc. Jpn. 30, 428 (1971); (b) S. Nakai and T. Sagawa, *ibid.* 26, 1427 (1969).
[37]R. Haensel, C. Kunz, T. Sasaki, and B. Sonntag, Phys. Rev. Lett. 20, 1436 (1968).
[38]A. Le Comte, A. Savary, M. Morlais, and S. Robin, Opt. Commun. 4, 296 (1971).
[39]R. Haensel, C. Kunz, and B. Sonntag, Phys. Rev. Lett. 20, 262 (1968).
[40]F. C. Brown, C. Gahwiller, A. B. Kunz, and N. O. Lipari, Phys. Rev. Lett. 25, 927 (1970).
[41]B. F. Sonntag, Phys. Rev. B 9, 3601 (1974).
[42]W. Gudat, C. Kunz, and H. Petersen, Phys. Rev. Lett. 32, 1370 (1974).
[43]S. T. Pantelides and F. C. Brown, Phys. Rev. Lett. 33, 298 (1974).
[44]A. A. Maiste, A. M. E. Saar, and M. A. Elango, Zh. Eksp. Teor. Fiz. Pis'ma Red. 18, 169 (1973) [JETP Lett. 18, 97 (1973)].
[45]T. Aberg and J. L. Dehmer, J. Phys. C 6, 1450 (1973).
[46]E. M. Rowe, R. A. Otte, C. H. Purett, and J. D. Steben, IEEE Trans. Nucl. Sci. NS-16, 159 (1969); E. M. Rowe and F. E. Mills, Part. Accel. 4, 211 (1973).
[47]S. A. Miller, Rev. Sci. Instrum. 39, 1923 (1968); D. L. Mickey, P. Zucchino, J. Born, and W. A. Smith, *ibid.* 41, 276 (1970).
[48]T. J. Moravec, Ph.D. thesis (University of Wisconsin, 1975) (unpublished).
[49]K. K. Rao and R. N. Dexter (technical note, University of Wisconsin, 1974) (unpublished); K. K. Rao, Ph.D. thesis (University of Wisconsin, 1975) (unpublished).
[50]B. W. Veal and A. P. Paulikas, Phys. Rev. B 10, 1280 (1974).
[51]P. C. Gibbons (private communication); J. R. Fields, S. E. Schnatterly, and P. C. Gibbons, Bull. Am. Phys. Soc. 20, 475 (1975).
[52]T. Tomiki, T. Miyata, and H. Tsukamoto, J. Phys. Jpn. 35, 495 (1973).
[53]C. Kunz, Comments Solid State Phys. 5, 31 (1973).
[54](a) S. P. Kowalczyk, F. R. McFeely, L. Ley, R. A. Pollak, and D. A. Shirley, Phys. Rev. B 9, 3573 (1974); (b) R. T. Poole, J. Liesegang, R. C. G. Leckey, and J. G. Jenkin, Chem. Phys. Lett. 23, 194 (1973).
[55]V. V. Nemoshkalenko, A. I. Senkevich, and V. G. Aleshin, Sov. Phys.–Doklady 17, 936 (1973).
[56]M. A. Butler, G. K. Wertheim, D. L. Rousseau, and S. Hufner, Chem. Phys. Lett. 13, 473 (1972).